

Pairing transition, coherence transition, and the irreversibility line in granular $\text{GdBa}_2\text{Cu}_3\text{O}_{7-\delta}$

J. Roa-Rojas, R. Menegotto Costa, and P. Pureur

Instituto de Física, Universidade Federal do Rio Grande do Sul, P.O. Box 15051, 91501-970 Porto Alegre, RS, Brazil

P. Prieto

Departamento de Física, Universidad del Valle A.A., 25360 Santiago de Cali, Colombia

(Received 14 September 1999)

We report on electrical magnetoconductivity experiments near the superconducting transition of a granular sample of $\text{GdBa}_2\text{Cu}_3\text{O}_{7-\delta}$. The measurements were performed in magnetic fields ranging from 0 to 500 Oe applied parallel to the current orientation. The results show that the transition proceeds in two steps. When the temperature is decreased we first observe the pairing transition, which stabilizes superconductivity within the grains at a temperature practically coincident with the bulk critical temperature T_c . Analysis of the fluctuation contributions to the conductivity shows that the universality class for this transition is that of the three dimensional (3D)-XY model in the ordered case, with dynamic critical exponent $z=3/2$. Close to the zero-resistance state, the measurements reveal the occurrence of a coherence transition, where the phases of the order parameter in individual grains become long-range ordered. The critical temperature T_{co} for this transition is close to the point where the resistivity vanishes. A strong enlargement of the fluctuation interval preceding the coherence transition is caused by the applied magnetic field. In this region, a 3D-Gaussian regime and an asymptotic critical regime were clearly identified. The critical conductivity behavior for the coherence transition is interpreted within a 3D-XY model where disorder and frustration are relevant. The irreversibility line is determined from magnetoconductivity measurements performed according to the zero-field-cooled (ZFC) and field-cooled data collected on cooling (FCC) recipes. The locus of this line coincides with the upper temperature limit for the fluctuation region above the coherence transition. The irreversibility line is interpreted as an effect of the formation of small clusters with closed loops of Josephson-coupled grains.

I. INTRODUCTION

Since the early studies on high-temperature superconductors (HTSC's), the pronounced granular character of sintered samples of these systems has been recognized.¹ In particular, their resistive transition shows a two-stage behavior,^{2,3} which is a distinctive characteristic of granular superconductors.⁴ At a higher temperature, which is practically coincident with the bulk critical temperature T_c , superconductivity stabilizes in homogeneous and mesoscopic regions of the sample (grains). The long-range superconducting state is achieved at a lower temperature T_{co} through a percolationlike process, which controls the activation of weak links between grains. A detailed study of this process, which has been called the "coherence transition," is given by Rosenblatt *et al.*⁵

At the coherence critical temperature T_{co} , the fluctuating phases of the Ginzburg-Landau order-parameter in each grain couple into a long-range ordered state and a zero-resistance state sets in. The relevant thermodynamics for this problem is obtained from the phase-glass Hamiltonian,⁶

$$H = - \sum_{i,j} J_{ij} \cos(\theta_i - \theta_j - A_{ij}) \quad (1)$$

where J_{ij} is the Josephson energy coupling between grains i and j , and θ_i denotes the phase of the order parameter in grain i . The gauge factor A_{ij} is given by

$$A_{ij} = \frac{2\pi}{\Phi_0} \int_i^j \vec{A} \cdot d\vec{l}, \quad (2)$$

where Φ_0 is the flux quantum and the line integral is evaluated between centers of grains i and j . The model represented by Eq. (1) belongs to the 3D-XY class with nontrivial (associated to frustration) disorder. Frustration is primarily introduced by a random distribution of the factors A_{ij} .⁷ The possibility for negative values of the J_{ij} couplings due to, e.g., the occurrence of π junctions, may also introduce frustration,⁸ much as in the conventional spin-glass models.⁹

Recently, we have presented electrical conductivity and specific-heat experiments,¹⁰ which give significant support to a description of the coherence transition as a genuine critical phenomenon. In this article, we report on detailed magnetoconductivity measurements at low applied fields in a $\text{GdBa}_2\text{Cu}_3\text{O}_{7-\delta}$ (GBCO) granular superconductor. The results show clearly that the transition to the superconducting state in this system is a two-stage process. In the normal phase, when the temperature approaches T_c from above, we observe that conductivity fluctuations scale as predicted by the Gaussian theory. Then, a crossover occurs to a behavior described by the full-dynamic 3D-XY universality class.

Below the pairing transition, and in the region approaching the zero-resistance state, our magnetoconductivity results can be fitted to power laws of a new reduced temperature, $\varepsilon_0 = [T - T_{co}(H)]/T_{co}(H)$, where $T_{co}(H)$ is almost coincident with the temperature where resistance vanishes. This behavior is an effect of thermal fluctuations that are precursory to the coherence transition. Large Gaussian and critical regimes related to the coherence transition could be discerned.

Measuring the magnetoresistivity according to the ZFC and FCC prescriptions,¹¹ we could also determine the irreversibility line. The locus of this line lies clearly above $T_{co}(H)$ and coincides approximately with the upper temperature limit for observing the fluctuation regimes related to the coherence transition.

II. EXPERIMENT

We have prepared a GBCO polycrystalline sample by the standard solid-state technique. Our procedure includes three intermediate grindings before the final sintering at 860 °C. Part of the obtained pellet was cut into a bar with dimensions $8 \times 2 \times 1$ mm for resistivity measurements, part was used for energy-dispersive x-ray analysis (EDAX) and electron microscopy, and part was ground again for powder x-ray diffraction. The EDAX analysis in several points of the sample surface indicated a rather homogeneous composition. Qualitative electron microscopy allowed the visualization of grains with average size of 5μ and ellipsoid shape, homogeneously distributed on the examined surface. The mass density of the sample was about 80% of the ideal value, and the x-ray spectrum displayed only the reflections expected for the GBCO orthorhombic structure. The obtained lattice parameters, $a = 3.905(8)$ Å, $b = 3.843(4)$ Å, and $c = 11.721(2)$ Å, are within the range of values reported in the literature.¹²

Resistivity measurements were performed using a low-frequency, low-current ac technique between the zero-resistance state and room temperature. Special care was taken in the temperature interval close to the transition in order to determine accurately the fluctuation contribution to the conductivity. Magnetic fields of 0, 5, 10, 20, 50, 100, 200, and 500 Oe were applied parallel to the current direction. Studies of the fluctuation magnetoconductivity were carried out when the field was applied in accordance to the FCC procedure. For determining the irreversibility line, experiments were performed sequentially according to the ZFC then the FCC recipes.

Temperatures were measured with a Pt sensor corrected for magnetoresistance effects that allows a resolution better than 2 mK. A large number of resistivity vs T points were recorded while the temperature was continuously increased or decreased across the transition in rates not exceeding 3 K/h. Using a numerical method, we could accurately determine the temperature derivative of the resistivity, $d\rho/dT$, in the interval near the transition.

III. RESULTS

Figure 1 shows the resistive transition of our granular GBCO sample in several applied fields. Panel 1(a) presents the resistivity versus temperature plots, whereas panel 1(b) depicts $d\rho/dT$ in the same temperature range. The two-stage nature of the superconducting transition in this systems is apparent from the results in both plots. The applied fields practically do not affect the shape of the curves in the temperature range above the main peak in $d\rho/dT$, whose position is denoted as T_P . This temperature, as shown in Fig. 2, is approximately coincident with the pairing critical temperature T_c . Below T_P , and down to the zero-resistance state,

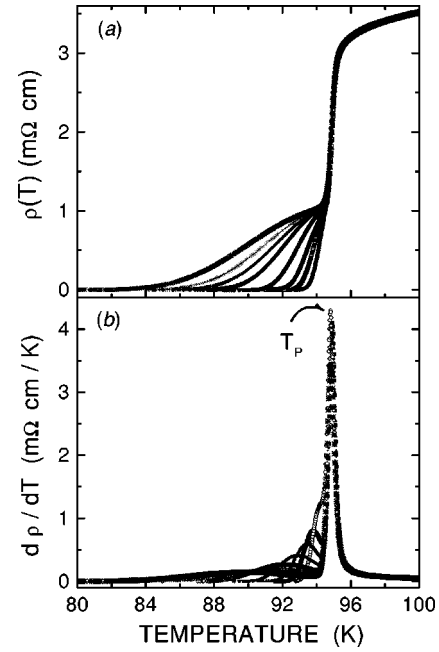


FIG. 1. Resistive transition of our granular GBCO sample in several fields applied parallel to the current, represented as (a) resistivity vs temperature and (b) $d\rho/dT$ vs temperature. The applied fields of 0, 5, 10, 20, 50, 100, 200, and 500 Oe regularly shift downwards the resistivity curves in the regime approaching the zero-resistance temperature.

the resistivity curves are dominated by effects related to granularity and depend strongly on the applied field.

The two-stage character of the resistivity transition in the granular HTSC is rendered still more evident by representing the data in terms of the quantity¹³

$$\chi_\sigma = -\frac{d}{dT} \ln \Delta\sigma, \quad (3)$$

where $\Delta\sigma$ is the fluctuation conductivity, given by

$$\Delta\sigma = \sigma - \sigma_R. \quad (4)$$

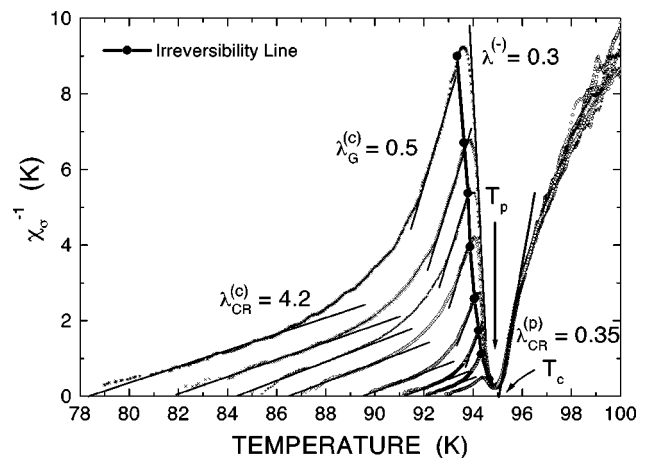


FIG. 2. Resistive transition for the same data of Fig. 1 represented as χ_σ^{-1} (see text) as a function of temperature. The straight lines are fits to Eq. (6) and are labeled by the respective critical exponents. The irreversibility temperatures for the studied fields are indicated by dots. The irreversibility line is a fit to Eq. (7).

In Eq. (4), $\sigma = 1/\rho$ is the measured conductivity and the subtracted regular term is estimated by extrapolating the high-temperature behavior $\sigma_R^{-1} = aT + b$, down to the region of the transition. Plots of χ_σ^{-1} as a function of T for several applied fields are shown in Fig. 2. There, one clearly observes distinctive behaviors in the temperature interval dominated by fluctuations in the normal phase above T_P (pairing transition), and in the region describing the approach to the zero-resistance state (coherence transition).

The main purpose of presenting the data in terms of χ_σ^{-1} is the study of the asymptotic critical fluctuation regimes. Indeed, assuming that $\Delta\sigma$ diverges as a power law when the temperature approaches T_c from above, that is,

$$\Delta\sigma \sim (T - T_c)^{-\lambda}, \quad (5)$$

we obtain that

$$\chi_\sigma^{-1} = \frac{1}{\lambda} (T - T_c). \quad (6)$$

Thus, as in the Kouvel-Fisher method¹⁴ for studying critical phenomena, the identification of a linear temperature region in χ_σ^{-1} allows the simultaneous determination of T_c and the critical exponent λ . In Fig. 2, straight-line fits to the χ_σ^{-1} data are shown.

Above T_P , we observe a power-law regime with the exponent $\lambda_{cr}^{(P)} = 0.35 \pm 0.02$. This value is consistent with expectations from the 3D-XY model,¹⁵ with dynamics given by the model E of Hohenberg and Halperin.¹⁶ This model describes the critical dynamics for the superfluid transition in helium, where the order parameter has two components and the density is a conserved quantity. The dynamical universality class of model E is also expected to be valid for the superconducting transition in extreme type-II systems.¹⁵ Above this genuine critical regime, it is possible to discern intervals dominated by Gaussian fluctuations,¹⁷ which are not addressed in this article.

When the temperature is decreased below the deep minimum where T_c is located, the χ_σ^{-1} data of Fig. 2 show the characteristic behavior of granular samples. First, χ_σ^{-1} increases steeply, such that its shape is nearly symmetrical with respect to the high-temperature side of the pairing transition, until a field-dependent maximum is attained. Then, χ_σ^{-1} decreases to zero at $T_{co}(H)$ with a curvature that is inverted when compared to that observed above T_c . This latter behavior results from the effect of phase fluctuations in the granular array above the coherence transition, and characterizes the so-called paracoherent state.⁵ When the field is increased, the width of the paracoherent fluctuation interval is correspondingly enlarged.

Two power-law regimes with field-independent exponents are identified in the paracoherent region of χ_σ^{-1} . Farther from T_{co} , and just below the granularity-induced maximum in χ_σ^{-1} , we obtain the exponent $\lambda_G^{(c)} = 0.53 \pm 0.03$. The identification of this regime becomes clearer when the field is increased above 20 Oe. Also evident is the asymptotic regime near $T_{co}(H)$, which is characterized by the exponent $\lambda_{cr}^{(c)} = 4.2 \pm 0.2$.

Figure 3(a) shows an example of magnetoresistance measurements performed in the ZFC and FCC conditions. The

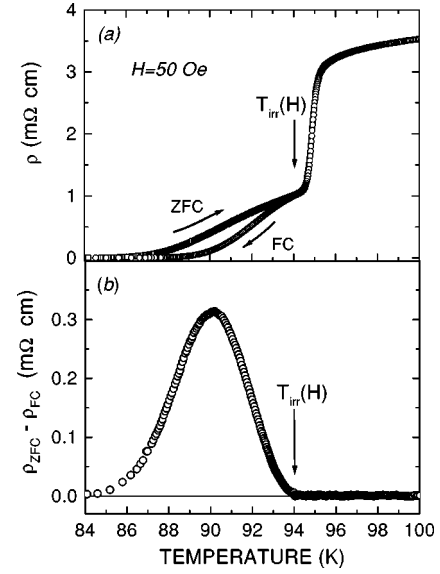


FIG. 3. (a) Representative resistivity experiments performed according to the ZFC (zero-field-cooled) and FCC (field-cooled cooling) prescriptions. The applied magnetic field is indicated. (b) Difference between results in panel (a) plotted as a function of temperature.

two curves split below a characteristic temperature $T_{irr}(H)$, which marks the onset of irreversible effects in the magnetotransport properties.¹¹ Figure 3(b) shows the difference between the FCC and ZFC magnetoresistances plotted as functions of temperature. Such plots allow an accurate determination of $T_{irr}(H)$. In the range of studied fields, the irreversibility temperatures so determined are coincident with those obtained from ZFC and FCC dc-magnetization measurements. The irreversibility temperatures vary with the applied field according to

$$\left(\frac{H}{H_0}\right) = \left[1 - \frac{T_{irr}(H)}{T_{irr}(0)}\right]^\gamma, \quad (7)$$

where $\gamma = 1.48 \pm 0.05$ and $H_0 = 63 \pm 2$ kOe.

The experimentally determined $T_{irr}(H)$, which are signaled by full circles in Fig. 2, are nearly coincident with the temperatures of the granular maximum in χ_σ^{-1} . This behavior clearly associates the onset of irreversibility effects in our granular superconductor with a threshold that marks the upper temperature limit of the paracoherent interval and separates single grain from collective grain responses in the fluctuation conductivity.

Rather interesting is the behavior of χ_σ^{-1} just above $T_{irr}(H)$ and up to the deep minimum where the pairing temperature is located. In this temperature range χ_σ^{-1} is approximately symmetrical with respect to the behavior observed in the normal phase just above T_c . Indeed, as shown in Fig. 2, in a certain region of this interval χ_σ^{-1} may be fitted to a straight line as $\chi_\sigma^{-1} = (1/\lambda^-)(T_c^- - T)$, where T_c^- is nearly coincident with T_c and $\lambda^- = 0.3$. This suggests an unexpected symmetry of the fluctuation-conductivity divergence around T_c . We note, however, that neither the λ^- regime nor the coherence transition have been identified in single

crystal samples,¹⁸ so that the λ^- regime might be related to finite-size effects in isolated grains of the ceramic HTSC samples.

IV. DISCUSSION

A. Pairing transition

The critical exponent for fluctuation conductivity is given by

$$\lambda = v(2 + z - d + \eta), \quad (8)$$

where v is the critical exponent for the coherence length, z is the dynamical critical exponent, d is the dimensionality, and η is the exponent of the order-parameter correlation function.

When the temperature approaches close enough to T_c , the critical thermodynamics of the superconducting transition is well described by the 3D-XY universality class.¹⁵ According to renormalization-group calculations,¹⁹ in this case one would expect $v=0.67$ and $\eta=0.03$. On the other hand, the theory of dynamical critical scaling^{16,20} predicts that $z=3/2$ for the superconducting transition. Substituting these values in Eq. (8), one obtains $\lambda \cong 0.35$, in agreement with our experimental finding for the asymptotic fluctuation regime precursor to the pairing transition, as shown in Fig. 2. This regime is observed in the whole range of applied fields and extends up to 0.85 K above T_c .

B. Coherence transition

The power law behavior of the conductivity, characterized by the exponent $\lambda_{cr}^{(c)}=4.2$, which governs the approach to the zero-resistance state at T_{co} , is interpreted as an effect of genuine critical fluctuations precursory to the coherence transition. In contrast to the critical regime near the pairing transition, the asymptotic critical interval in the paracoherent state extends to several K and enlarges when the field magnitude is increased. This is indeed suggestive of a percolationlike transition associated to the connective nature of the granular array in ceramic HTSC's. In this case,²¹ as well as in other disordered and frustrated systems,²² the critical exponent for the correlation length is found to be $v \cong 4/3$. From Eq. (8), where we put $d=3$ and assume $\eta \cong 0$, the conductivity exponent $\lambda_{cr}^{(c)}=4.2$ corresponds to $z \cong 4.1$.

The whole picture emerging from our experiments is consistent with results obtained²³ from I-V isothermal measurements in polycrystalline $\text{YBa}_2\text{Cu}_3\text{O}_{7-\delta}$ (YBCO), and agrees with conclusions of a recent Monte Carlo study by Wengen and Young,²⁴ based on the 3D-XY phase-glass Hamiltonian of Eq. (1). These authors found that in both the gauge-glass (disorder introduced by a random distribution in the gauge factors A_{ij}) and chiral-glass (disorder due to random sign distribution in the bonds J_{ij}) versions of the model based on Eq. (1), the critical exponents are $v \cong 1.3$ and $z \cong 3.1$. According to Eq. (8), this yields a conductivity exponent $\lambda_{cr}^{(c)} \cong 3$. This value has been found in several experiments performed in zero applied field.^{10,13,25,26} However, in the presence of a small field or when the width of the paracoherent critical interval is large enough, the asymptotic conductivity regime generally corresponds to $\lambda_{cr}^{(c)} \cong 4$.^{13,26} This indicates

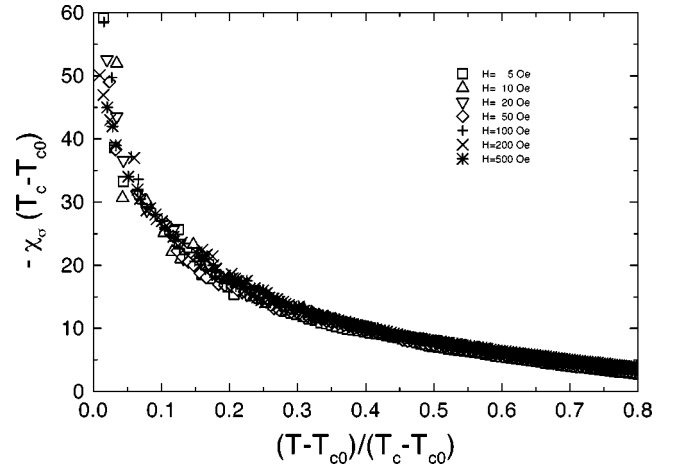


FIG. 4. Scaling of the fluctuation magnetoconductivity results of Fig. 2 between T_{co} and T_c , in accordance to Eq. (12).

that the dynamical universality class of the coherence transition in the presence of a small magnetic field is closer to that of a spin glass, where one indeed expects²⁷ $z \cong 4$.

Farther from T_{co} , and just below the maximum in χ_{σ}^{-1} , the regime described by the exponent $\lambda_G^{(c)} \cong 0.5$ is likely due to three-dimensional Gaussian fluctuations. Using the mean-field values $v=0.5$, $\eta=0$, and $z=2$ in Eq. (8), one reproduces the measured value of $\lambda_G^{(c)}$. We notice that this is probably the first identification of a Gaussian regime corresponding to a vortex-glass-like transition. Such fluctuations were searched for unsuccessfully in I-V experiments in YBCO thin films.²⁸ It is also interesting to note that the fluctuation spectrum is isotropic in the whole paracoherent interval, in spite of the strong planar anisotropy of the intra-grain superconductivity.

The shape of the χ_{σ}^{-1} results of Fig. 2 in the paracoherent region strongly suggests that the whole measurements may be scaled into a single curve.

The scaling behavior proposed for the fluctuation conductivity close to a vortex-glass transition is given by²⁹

$$\Delta \sim H^{-1/2(2+z-d)} S_{\pm} \left(\frac{\varepsilon_0}{H^{1/2v}} \right), \quad (9)$$

where $\varepsilon_0 = (T - T_{co})/T_{co}$, and S_{\pm} are scaling functions above and below T_{co} , respectively.

Assuming, following Fisher *et al.*,³⁰ that

$$[T_c - T_{co}(H)] \sim H^{1/2v} \quad (10)$$

and using the scaling variable introduced by Kötzer *et al.*,³¹

$$\tau = \frac{T - T_{co}(H)}{T_c - T_{co}(H)}, \quad (11)$$

we derive that

$$\frac{d}{d\tau} \ln S_{+}(\tau) = \chi_{\sigma} [T_c - T_{co}(H)] \quad (12)$$

in the fluctuation region above the coherence transition and below the pairing transition. Figure 4 shows a plot of $\chi_{\sigma} [T_c - T_{co}(H)]$ vs τ determined from the results presented

in Fig. 2. Good scaling is indeed obtained in most of the range $[0,1]$ for the variable τ . Deviations occur close to the high-temperature end because of the steep variation of χ_σ^{-1} above the irreversibility line in Fig. 2, where data scale rather with T_c , as discussed in the last paragraph of Sec. III.

C. Irreversibility line

The de Almeida-Thouless-like behavior of the irreversibility line in our granular HTSC at low applied fields may be explained by the phase-glass model of Eq. (1). The coincidence of the irreversibility temperature at a given field with the maximum in χ_σ^{-1} , signaling the high-temperature limit of the paracoherent fluctuation interval, is a clear indication that the onset of irreversibility effects is a threshold separating single-grain from collective-grain behavior. The Hamiltonian of Eq. (1) predicts that when loops of weakly coupled grains are formed, frustration may occur since the coupling energies between all pairs of grains cannot be simultaneously minimized in the presence of the random gauge factors A_{ij} .^{6,7} As a consequence, the state of a small aggregate of interacting grains becomes highly degenerate with many nearly equivalent low-energy configurations. Irreversible effects occur when the system evolves through the rugged landscape characteristic of the phase space in disordered and frustrated systems.⁹ Thus, the irreversibility line at low fields in granular superconductors is a consequence of the stabilization of relatively small aggregates of coupled grains, and do not represent necessarily a phase transition. In other terms, the irreversibility line is related to the onset of short-range ordering, in contrast to the percolationlike coherence transition that is achieved when an (ideally) infinite cluster of coupled grains is formed in the sample.

V. CONCLUSIONS

Our low-field magnetoconductivity results in a granular GBCO superconductor show that the resistive transition in this system is a two-stage process. When the superconducting state is approached from above we first observe the occurrence of a pairing transition, which stabilizes the condensate within the grains at a critical temperature T_c close to that of a bulk specimen. This transition is preceded by large regimes dominated by fluctuations of the order parameter amplitude. Immediately above T_c a full dynamic 3D-XY fluc-

uation regime, with $z=3/2$, is clearly identified. This regime extends up to 0.85 K above T_c , and is robust against magnetic fields applied parallel to the current in the range 0–500 Oe.

The genuine superconducting state with zero-resistance stabilizes at the coherence transition that occurs at a lower temperature T_{co} , where a long-range-ordered state for the phase of the order parameter is established in the whole granular array. The approach to the zero-resistance state is dominated by strong fluctuations of the phase of the order parameter of individual grains. Extended power law regimes corresponding to 3D-Gaussian and critical fluctuations are identified in the magnetoconductivity experiments. The obtained exponent in the asymptotic critical regime indicates that the static and dynamic universality classes for the coherence transition is that of the 3D-XY model described by the phase-glass Hamiltonian of Eq. (1), where the disorder is nontrivial (accompanied by frustration) and critically relevant. A scaling analysis of the conductivity in the interval between T_{co} and T_c shows that the coherence transition in our homogeneously granular superconductor fits into the more general framework of the vortex-glass theory.

Magnetoconductivity measurements performed according to the ZFC and FCC prescriptions allowed the determination of the irreversibility line. The locus of this line lies clearly above the zero-resistance temperatures and coincides approximately with the high-temperature limit for the fluctuation region above the coherence transition. This indicates that the low-field irreversibility line in granular superconductors is a threshold separating single-grain from collective-grain behavior and is related to the formation of small clusters with closed loops of Josephson-coupled grains.

ACKNOWLEDGMENTS

We are indebted to Dr. Miguel A. Gusmão for a careful reading of the manuscript and to Dr. Enzo Granato for illuminating discussions. We also acknowledge Dr. M. Z. Vasconcellos for the EDAX analysis and Claudia M. Haetinger for help with the text. This work was partially supported by the Brazilian Ministry of Science and Technology under Contract PRONEX/FINEP/CNPq No. 41.96.0907.00. One of us (J.R.R.) received support by CNPq (Brazil) and COLCIENCIAS (Colombia).

¹K. A. Müller, M. Takashige, and J. G. Bednorz, *Phys. Rev. Lett.* **58**, 1143 (1987).

²A. Gerber, T. Grenet, M. Cyrot, and J. Beille, *Phys. Rev. Lett.* **65**, 3201 (1990).

³P. Pureur, J. Schaf, and J. V. Kunzler, in *Progress in High Temperature Superconductivity*, edited by R. Nicolisky, R. A. Barrio, O. F. de Lima, and R. Escudero (World Scientific, Singapore, 1988), Vol. 9, p. 137.

⁴See *Inhomogeneous Superconductors – 1979*, edited by D. U. Gubser, T. L. Francavilla, S. A. Wolf, and J. R. Leibowitz, AIP Conf. Proc. No. 58 (AIP, New York, 1980).

⁵J. Rosenblatt, in *Percolation, Localization and Superconductivity*, Vol. 109 of *NATO Advanced Study Institute, Series B: Physics*, edited by A. M. Goldman and S. A. Wolf (Plenum, New York,

1984), p. 431; J. Rosenblatt, P. Peyral, A. Raboutou, and C. Lebeau, *Physica B* **152**, 95 (1988).

⁶W. Y. Shih, C. Ebner, and D. Stroud, *Phys. Rev. B* **30**, 134 (1984).

⁷C. Ebner and D. Stroud, *Phys. Rev. B* **31**, 165 (1985).

⁸H. Kawamura and M. S. Li, *J. Phys. Soc. Jpn.* **66**, 2110 (1997).

⁹See, for example, K. Binder and A. P. Young, *Rev. Mod. Phys.* **58**, 801 (1986).

¹⁰A. R. Jurelo, I. Abrego-Castillo, J. Roa-Rojas, L. M. Ferreira, L. Ghivelder, P. Pureur, and P. Rodrigues, Jr., *Physica C* **311**, 133 (1999).

¹¹J. F. Carolan, W. N. Hordy, R. Krahn, J. H. Brewer, R. C. Thompson, and A. C. D. Chaklader, *Solid State Commun.* **54**, 717 (1987).

- ¹²R. M. Hazen, in *Physical Properties of High Temperature Superconductors*, edited by D. M. Ginsberg (World Scientific, Singapore, 1990), Vol. 2, p. 121.
- ¹³P. Pureur, R. Menegotto Costa, P. Rodrigues, Jr., J. Schaf, and J. V. Kunzler, Phys. Rev. B **47**, 11 420 (1993).
- ¹⁴J. S. Kouvel and M. E. Fisher, Phys. Rev. **136**, A1616 (1964).
- ¹⁵C. J. Lobb, Phys. Rev. **36**, 3930 (1987).
- ¹⁶P. C. Hohenberg and B. I. Halperin, Rev. Mod. Phys. **49**, 435 (1977).
- ¹⁷P. P. Freitas, C. C. Tsuei, and T. S. Plaskett, Phys. Rev. B **36**, 833 (1987).
- ¹⁸R. Menegotto Costa, P. Pureur, M. Gusmão, S. Senoussi, and K. Behnia, Solid State Commun. **113**, 23 (2000).
- ¹⁹J. C. Le Guillou and J. Zinn-Justin, Phys. Rev. B **21**, 3976 (1980).
- ²⁰J. Lidmar, M. Wallin, C. Wengel, S. M. Girvin, and A. P. Young, Phys. Rev. B **58**, 2827 (1998).
- ²¹C. Lebeau, A. Raboutou, P. Peyral, and J. Rosenblatt, Physica B **152**, 100 (1988).
- ²²I. A. Campbell, Phys. Rev. B **37**, 9800 (1988).
- ²³R. J. Joshi, R. B. Hallock, and J. A. Taylor, Phys. Rev. B **55**, 9107 (1997).
- ²⁴C. Wengel and A. P. Young, Phys. Rev. B **56**, 5918 (1997).
- ²⁵P. Peyral, C. Lebeau, J. Rosenblatt, A. Raboutou, C. Perrin, O. Pena, and M. Sergent, J. Less-Common Met. **151**, 49 (1989).
- ²⁶A. R. Jurelo, J. V. Kunzler, J. Schaf, P. Pureur, and J. Rosenblatt, Phys. Rev. B **56**, 14 815 (1997).
- ²⁷A. Zippelius, Phys. Rev. B **29**, 2717 (1984); A. T. Dorsey, M. Huang, and M. P. A. Fisher, *ibid.* **45**, 523 (1992).
- ²⁸M. Friesen, J. Deak, L. Hou, and M. McElfresh, Phys. Rev. B **54**, 3525 (1996).
- ²⁹N. C. Yeh, D. S. Reed, W. Jiang, U. Kriplani, F. Holtzberg, A. Gupta, B. D. Hunt, R. P. Vasquez, M. C. Foote, and L. Bajuk, Phys. Rev. B **45**, 5654 (1992).
- ³⁰D. S. Fisher, M. P. A. Fisher, and D. A. Huse, Phys. Rev. B **43**, 130 (1991).
- ³¹J. Kötzler, M. Kaufmann, G. Nakielski, R. Behr, and W. Assmus, Phys. Rev. Lett. **72**, 2081 (1994).